 https://doi.org/10.3311/PPci.21155

Periodica Polytechnica Civil Engineering, 67(2), pp. 444–456, 2023

Size Effect on Flexural and Fracture Properties of Polypropylene Fiber-reinforced Engineered Cementitious Composite

Alireza Hosseini Mehrab[1], Seyedmahdi Amirfakhrian[1], M. Reza Esfahani[1*]

[1] Department of Civil Engineering, Ferdowsi University of Mashhad, Azadi Square, 9177948974 Mashhad, Iran
[*] Corresponding author, e-mail: esfahani@um.ac.ir

Received: 10 September 2022, Accepted: 12 January 2023, Published online: 30 January 2023

Abstract

The size effect on flexural properties and fracture behavior of polypropylene fiber-reinforced engineered cementitious composite (PPFECC) containing local waste materials was investigated. Geometrically similar notched beams with dimensions of 190 × 70 × 70 mm (small), 380 × 70 × 140 mm (medium), and 760 × 70 × 280 mm (large) were tested using three-point bending to study the size effect on flexural properties, toughness, and fracture behavior in PPFECC and the influence of tensile ductility of PPFECC on the size effect parameter. Two PPFECC mixtures containing 1% (PPFECC1) and 2% (PPFECC2) volume fraction of polypropylene fibers were prepared. The results indicated clear size effect on ductility, flexural strength, normalized deflection, normalized toughness, and fracture energy for both PPFECCs. The flexural properties and fracture behavior in PPFECC1 were more sensitive to the size effect parameter due to its lower tensile ductility compared to PPFECC2. Moreover, according to Bažant's size effect curve, the behavior of notched beams in PPFECC2 with higher tensile ductility was closer to the strength criterion compared to PPFECC1.

Keywords

size effect, engineered cementitious composite, fracture energy, toughness, ductility

1 Introduction

During the last decades, the engineered cementitious composite (ECC) has drawn the attention of many scholars and designers in various structures, such as high-rise buildings, bridge decks, tunnels, and highways, in different parts of the world [1–4]. ECC is a particular class of ultra-high ductile fiber-reinforced cementitious composite, which exhibits its significant performance in the strain-hardening stage due to triggering multiple cracks with width less than 100 μm while keeping the volume content of randomly distributed short fibers no more than 2% [3, 5]. ECC, also called bendable concrete, is recognized for its high tensile strain capacity and excellent crack control characteristics because of the micromechanical tailoring and fracture mechanics principles used in this material [6–8].

The classical ECC comprises common materials such as cement binder, fly ash, fine silica sand, polyvinyl-alcohol (PVA) fibers, water, and superplasticizer [7, 8]. Most studies were focused on determining the mechanical properties, fracture behavior, durability, ductility, and rheological characteristics of ECC containing these common materials [5, 6, 8]. However, some scholars recommended using alternative materials in ECC composition since some materials mentioned above are costly and unavailable in different areas, particularly in some developing countries [7–11]. Fischer and Li [12] reported that the tremendous cost of classical ECC restricted its structural applications. In some studies, the PVA fiber was replaced by other types of polymer fibers in ECC due to its high-cost [8, 9]. Among these polymer fibers, polypropylene fiber was mostly used for reinforcing ECC by many scholars due to its low-cost and appropriate properties [8, 9].

Moreover, the unavailability, high-cost, and complex production of fine silica sand led scholars to use natural river sand, sea sand, and stone powder in ECC [13–15]. Different pozzolanic materials such as silica fume, ground granulated blast furnace slag, metakaolin, electric arc furnace dust, and rice husk ash were also employed in ECC not only to improve the quality but result in an economical and green ECC [6, 13-16]. According to the experimental study conducted by da Costa et al. [8], the incorporation

Cite this article as: Hosseini Mehrab, A., Amirfakhrian S., Reza Esfahani, M. "Size Effect on Flexural and Fracture Properties of Polypropylene Fiber-reinforced Engineered Cementitious Composite", Periodica Polytechnica Civil Engineering, 67(2), pp. 444–456, 2023. https://doi.org/10.3311/PPci.21155

of polypropylene fibers as the replacement for PVA fibers and rice husk ash as the replacement for portion of cement led to the development of ECC with appropriate mechanical and durability properties. Zhu et al. [9] conducted an experimental investigation on the effects of polypropylene fibers and superfine river sand as substitutes for PVA fibers and fine silica sand, respectively, in ECC. They reported that using polypropylene fibers and superfine river sand in ECC catered to the demands of many concrete structures and demonstrated outstanding potential for large-scale applications of deformable cementitious composites [9]. Yao et al. [14] reported that adding metakaolin could increase the durability of ECC. Additionally, they observed that the sea sand showed a highly positive influence on the mechanical performance of ECC [14]. Overall, many efforts have been devoted to numerically and experimentally investigating the mechanical properties, fracture characteristics, resistance, and durability of various ECC in the last decades, and the significant characteristics of this novel structural material have drawn the attention of researchers and structural engineers who wish to utilize this material in structural applications.

However, the characteristics of different ECC might vary due to the size effect parameter. The study on the size effect of ECC is minimal. Several scholars attempted to study the size effect on mechanical properties and fracture behavior of classical ECC [1, 3, 17, 18]. Lepech and Li [17] experimentally investigated the size effect on the flexural strength of ECC containing commonly used materials with three levels of tensile strain capacity (1%, 3%, and 5%). They found that the size effect on ECC is inappreciable since the ECC due to the significant tensile ductility and the development of multiple cracks can suppress the fracture localization and shift the brittle fracture mode to ductile mode within the four-point bending unnotched beams [17]. However, they have only investigated the size dependency of flexural properties in classical ECC. Asano et al. [18] observed that the bending strength increases as the size of specimens decreases in ECC containing PVA fiber [18]. However, their investigation was only on four-point bending intact beams. Erdem [1] experimentally studied the size effect on the residual properties of classical ECC subjected to high temperatures up to 800 °C and pointed out that as the size of specimens and the exposure temperature increase, the stiffness and compressive strength decrease. However, this research only studied the mechanical properties, and the size dependency of flexural behavior and fracture parameters was neglected. Moreover, no-evident study was reported to investigate the size effect on ECC with alternative materials such as polypropylene fibers, pozzolanic materials, and local waste compositions.

Therefore, considering the insufficient studies in determining the size effect on flexural properties and fracture behavior in ECC, particularly in ECC with local waste and low-cost materials, effort has been made in this experimental study to investigate the size effect on flexural characteristics, toughness, and fracture properties of eco-friendly polypropylene fiber-reinforced ECC (PPFECC) with local waste constituent materials. Two PPFECC mixtures containing 1% and 2% volume fractions of polypropylene fibers were prepared. The size effect of these two mixtures was studied on geometrically similar notched beams with dimensions of 190 × 70 × 70 mm (small), 380 × 70 × 140 mm (medium), and 760 × 70 × 280 mm (large) under the three-point bending test.

2 Theoretical review of size effect parameter

Employing the behavior of small-size laboratory specimens in modeling and designing large structures is the most compelling reason that shows the importance of the size effect parameter. Several scholars proposed methods to investigate this parameter [19–24]. Among them, two approaches were widely used in various studies to explain the size effect on material strength, including statistical and deterministic [25–27]. The statistical approach represents Weibull's theory, while the deterministic approach, based on fracture mechanics, represents Bažant's theory [19, 27].

Weibull's theory is simple and easy to use since the size effect sources are not explained. However, applying this approach to quasi-brittle materials such as concrete and cementitious composites faces several objections that restrict the further use of this theory [28]. On the contrary, Bažant's theory is proposed especially to investigate the size effect on concrete and quasi-brittle materials [19]. Bažant presented this theory according to the deterministic approach using the fracture mechanics method for concrete and cementitious composites [21]. In this theory, one of the major influences of the size effect parameter is the decrease of strength due to the increase in structure size. A series of geometrically similar structures of different sizes were used to investigate the size effect parameter based on a characteristic dimension (D) of structures (Fig. 1).

This characteristic dimension, D, represents the depth (d) in notched beams [20]. In these beams, the width (b) is constant. The nominal stress at failure (σ_{Nu}), which is also called the nominal strength, is described by

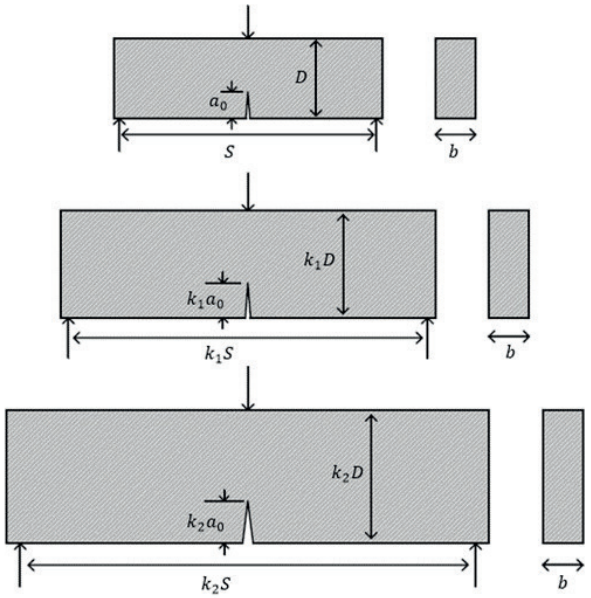

Fig. 1 Geometrically similar notched beams (k_1 and k_2 are constant) [20]

$$\sigma_{Nu} = \frac{c_n P_u}{bD}, \tag{1}$$

where P_u is the peak load, b is the constant width of structures, and c_n is a coefficient that exhibits the type of structure [20]. Based on the assumption that the dissipated fracture energy at failure is smooth and it is the function of the size of fracture process zone and the beam dimensions, Bažant [19, 20] demonstrated that the nominal strength for distinct sizes could be expressed as follows:

$$\sigma_N = \frac{Bf_t}{\sqrt{1+\beta}} = \frac{Bf_t}{\sqrt{1+D/D_0}}, \tag{2}$$

where f_t is the size-independent tensile strength, B is a dimensionless constant parameter based on plastic limit analysis, β is the brittleness number and equal to the ratio of D/D_0, D is the size of specimen, and D_0 is the characteristic length based on structural geometry [20, 27]. The nominal stress is constant regardless of structural size in classical theories such as strength and yield criteria. Based on these criteria, all geometrically similar structures fail at the same nominal strength and exhibit no size effect [29]. As shown in Fig. 2, the size effect is not considered in the strength criterion, and the horizontal dashed line depicts it. This criterion is appropriate for ductile and small-size laboratory specimens. On the other hand, the nominal strength demonstrates significant size effect based on linear elastic fracture mechanics (LEFM). This approach is illustrated by the inclined dashed line with slope –1/2 in Fig. 2. This criterion is appropriate for brittle and large structures [19, 20]. The curved line in Fig. 2 shows nonlinear fracture mechanics (NLFM).

This curved line indicates the transitional behavior of quasi-brittle materials such as concrete. According to this curve, when the size of structure is large, its behavior approaches the LEFM, and when the size of structure is small, its behavior is close to the strength criterion [29]. Apart from the size effect on strength, there is another size effect, which is on the ductility of the structures, and it can be characterized by the deformation at which the structure fails under a given type of loading [19]. This size effect primarily influences the descending branch or the post-peak response of the load-deflection curve. Fig. 3 illustrates the stress-relative deflection curves of geometrically similar structures with different sizes. In this curve, the relative deflection can be explained by u/D ratio, in which the is the deflection and D is the characteristic dimension of the structures [19]. It can be seen in Fig. 3 that the post-peak response for small structures descends slowly. In comparison, it descends steeper as the size of specimens increases. It has even shown a snapback for sufficiently large structures [21]. Since the large structures have more considerable strain energy to propagate the failure zone and overcome the fracture process zone compared to small structures, the large structures show smaller ductility than the small ones [20].

The other parameter which is size-dependent is the flexural behavior (f) of concrete that alters with the dimensions of the structures (D) [27, 30]. This size effect was studied by investigating equivalent bending strength, normalized

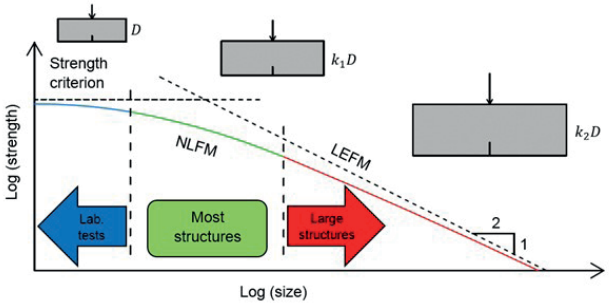

Fig. 2 Size effect for a series of geometrically similar structures

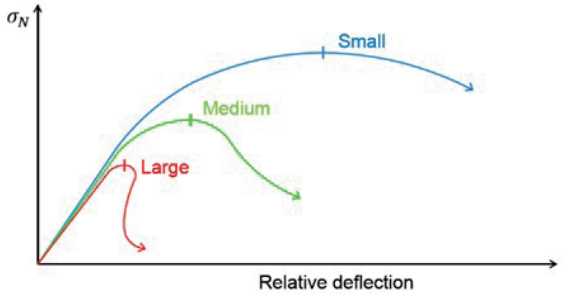

Fig. 3 Load-deflection curves of geometrically similar structures

deflection, and normalized toughness of notched beams [30, 31]. The size variations in these parameters with the dimensions of the structures are such that the equivalent bending strength, normalized deflection, and normalized toughness reduce when the size of specimens enhances. To investigate the size effect on flexural behavior, the equivalent bending stress-normalized deflection curves should be determined [27, 31]. The equivalent bending strength (f_j) could be explained as follows:

$$f_j = \frac{3P_j S}{2b\left(d-a_0\right)^2}, \tag{3}$$

where P_j is the applied load, S is the span of the notched beams, b is the beam width, d is the beam depth, and a_0 is the length of notch. Two important points in describing the equivalent bending strength are the limit of proportionality (LOP) and the modulus of rupture (MOR). The LOP is defined as the point corresponding to the highest load value in the deflection interval of 0.08 mm, and the MOR is the point corresponding to the maximum equivalent bending strength [27]. The normalized deflection can be defined by δ/S ratio, in which δ is the deflection, and the S is the span of the notched beams. Moreover, the normalized toughness (T_N) can be determined as the area below the equivalent bending strength (f_j) versus normalized deflection (δ/S) up to a specified point [30].

The fracture energy (G_F) of concrete also depends on the shape and the size of specimens [32–35]. This size dependency may be due to the existence of fracture process zone in front of the extending crack and the unwanted energy absorption outside the fracture process zone [20, 36]. This unwanted energy absorption increases as the size of structures enhances. The G_F could be determined as follows:

$$G_F = \frac{w_0 + 2P_w\delta_0}{b\left(d-a_0\right)}, \tag{4}$$

where w_0 is the total area below the load-deflection curve, the equivalent force P_w represents the influence of concrete beam self-weight, and δ_0 is the displacement at zero loading [20]. Additionally, the parameters b, d, and a_0 are the beam width, the beam depth, and the notch depth, respectively. The $b(d - a_0)$ is the initial ligament area. In the current study, the equation, $w_0 + 2P_w\delta_0$, is illustrated with w_t. Some scholars reported that experimental errors such as testing equipment, friction of supports, weight of specimens, bulk energy dissipation, and cutting the tail of load-deflection curve are the reasons for the unwanted energy absorption [36–38]. By considering these errors in calculating fracture energy, the fracture energy may be more or less size independent [20]. However, the fracture energy is still size dependent [20].

3 Experimental program

3.1 Materials and mix proportions

Type II Portland cement supplied from Mashhad Cement Co. (Mashhad, Iran) was used in the mixtures. Silica fume supplied from Zhikava Co. (Mashhad, Iran) was employed as a replacement for 10% of the weight of cement. Stone sludge powder from Kara Powder Co. (Mashhad, Iran) with a maximum particle size of 0.2 mm was used as fine aggregates instead of fine silica sand. Moreover, electric arc furnace dust collected from the Khorasan steel complex (Neyshabur, Iran) was utilized as a replacement for 26% of the weight of cement in both mixtures. To reduce the water content, keep the workability, and achieve a proper performance, a carboxylate-based superplasticizer supplied by Zhikava Co. (Mashhad, Iran) with a specific gravity of 1.08 g/cm^3 was employed. The polypropylene fibers from Zhikava Co. (Mashhad, Iran) were used in the mixtures. The chemical and physical properties of cement, silica fume, and sludge stone powder were provided by the suppliers. The properties of electric arc furnace dust were provided by Sabzi et al. [39]. These material properties are shown in Table 1. In addition, the characteristics of polypropylene fibers provided by the supplier are illustrated in Table 2. Fig. 4 shows each of the materials used in the mixtures.

Two ECC mixtures were prepared, including 1% (PPFECC1) and 2% (PPFECC2) volume fractions of polypropylene fibers. Table 3 depicts these two mix designs.

3.2 Preparation

For the production of ECC mixtures, the water and the superplasticizer were mixed. Then the silica fume was gradually added to the blend of water and superplasticizer for 2 minutes. Afterward, the stone sludge powder, electric arc furnace dust, and cement were employed in the blend and mixed for 4 minutes. Finally, the polypropylene fibers were gradually employed in the mixture for 2 minutes, and the mixing continued for 5 minutes to have uniform dispersion of polypropylene fibers. After the production, the ECC mixtures were cast in the molds. Then the samples were demolded within 24 hours. All the specimens were cured for 28 days.

Table 1 Chemical and physical properties of materials

Chemical compositions (wt. %)	Materials			
	PC	SF	SSP	EAFD
SiO_2	21.0	93.6	0.65	4.5
Al_2O_3	4.6	1.3	0.14	0.3
Fe_2O_3	3.9	0.3	0.11	53.3
CaO	62.5	0.49	53.48	10.5
MgO	2.9	0.97	0.95	4.0
SO_3	2.0	0.1	-	0.6
Na_2O	0.5	0.31	0.13	3.4
K_2O	0.45	1.01	0.01	5.7
L·O·I	1.4	-	43.88	15.5
SiC	-	0.5	-	-
C	-	0.3	-	-
P_2O_5	-	0.16	0.029	-
TiO_2	-	-	0.016	0.1
MnO	-	-	0.001	-
Physical properties				
Specific gravity (g/cm^3)	3.15	2.21	2.7	4
Compressive strength, 28 days (MPa)	49.5	-	-	-
Autoclave expansion (%)	0.08	-	-	-
Fineness, Blaine test (cm^2/g)	3200	-	-	-

Notes: PC: Portland cement; SF: silica fume; SSP: stone sludge powder; EAFD: electric arc furnace dust

3.3 Test methods

Three-point bend notched beams with geometrically similar dimensions were made following the RILEM TC-89 [40] to study the size effect on flexural properties, toughness, and fracture behavior in the mixtures. For each mix design, three notched beams from each dimension were made.

Table 2 Characteristics of polypropylene fibers

Specific gravity (g/cm^3)	Elastic modulus (GPa)	Tensile strength (MPa)	Elongation (%)	Length (mm)	Diameter (mm)
0.91	6.0	400	80	12	0.035

Three sizes were used for the depth of notched beams (d), 70, 140, and 280 mm. The width (b) was constant and equal to 70 mm in all notched beams. In these beams, the width of notches was 3 mm. Other beam geometries, such as the notch depth (a_0), the beam span (S), and the beam length (L), are illustrated in Fig. 5.

All notched beams were loaded based on RILEM TC-89 [40], in which the maximum load should reached nearly about 5 minutes. Therefore, the loading rate was set to 0.25 mm/min. The size effect on strength and ductility was investigated through Bažant's size effect law and Bažant's stress-relative deflection curve, respectively [19, 21]. The size effect on flexural behavior and toughness was investigated through BS EN 14651 [41] and ASTM C1609 [42]. The size effect on fracture energy was studied using RILEM TC-50 FMC [43]. The test setup is shown in Fig. 6. To determine the mechanical parameters, the compressive strength (f_c) was examined on the cubic specimens with dimensions of 100 × 100 × 100 mm, according to BS EN 12390 [44]. The flexural strength (f_r) was tested on 300 × 100 × 50 mm beams according to ASTM C78 [45]. Also, the splitting tensile strength (f_t) was studied on 100×200 mm cylindrical specimens based on ASTM C496 [46]. Both specimens are shown in Fig. 7. Three specimens for each of mechanical tests were prepared and tested.

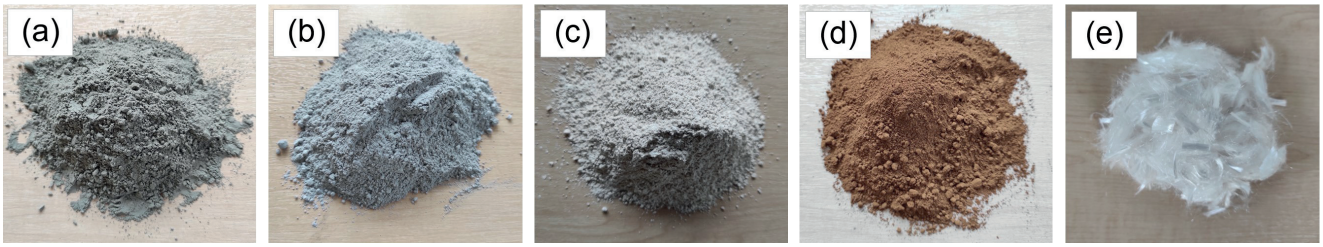

Fig. 4 Materials: (a) Portland cement, (b) silica fume, (c) stone sludge powder, (d) electric arc furnace dust, and (e) polypropylene fibers

Table 3 Mix proportions of ECC mixtures

Mixtures	PC (kg/m^3)	SF (kg/m^3)	SSP (kg/m^3)	EAFD (kg/m^3)	SP (kg/m^3)	Water (kg/m^3)	Volume contents of fibers, V_{pf} (%)	Unit weight (kg/m^3)	Slump flow (mm)
PPFECC1	496	264	596	132	21	452	1	1962	380
PPFECC2	496	264	596	132	25	452	2	1967	340

Notes: PC: Portland cement; SF: silica fume; SSP: stone sludge powder; EAFD: electric arc furnace dust, SP: superplasticizer

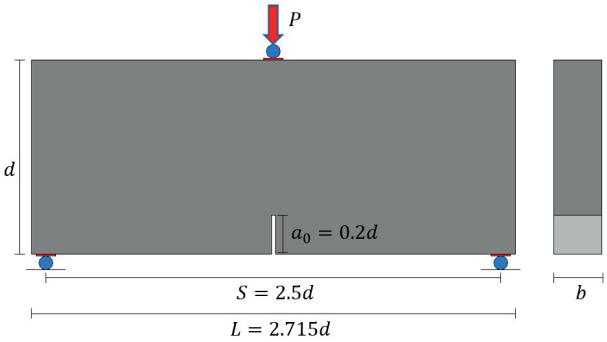

Fig. 5 Dimensions of geometrically similar notched beams

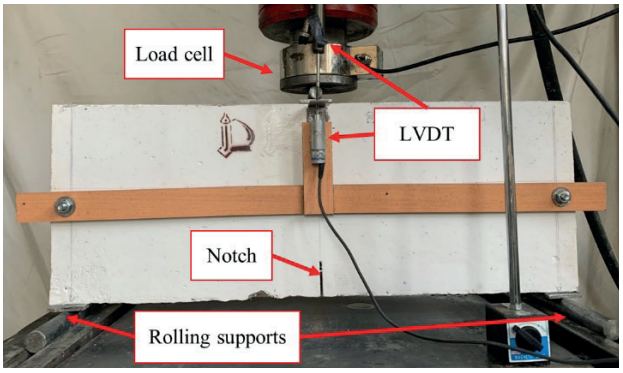

Fig. 6 Test setup of geometrically similar notched beams

Fig. 7 Specimens under testing: (a) compressive, (b) flexural, and (c) tensile

4 Results and discussion

4.1 Analysis of mechanical properties

Table 4 demonstrates the average values of mechanical properties of PPFECCs. Besides, the load-deflection curves of 300 × 100 × 50 mm beams are demonstrated in Fig. 8. As shown in Table 4, although the compressive strength (f_c) of PPFECC2 was lower than that of PPFECC1, the tensile strength (f_t) and flexural strength (f_r) of PPFECC2 were higher than PPFECC1. This result shows that the tensile ductility of PPFECC2 was higher than that of PPFECC1. It can also be seen in Fig. 8 and Fig. 9 that the strain-hardening response accompanied by multiple micro and macro cracks was developed on both PPFECC mixtures. However, the PPFECC2 sustained greater deflections and showed higher load-bearing capacity than PPFECC1. Therefore, the tensile capacity of PPFECC2 was more than that of PPFECC1.

Table 4 Mechanical properties of PPFECC mixtures

Mixture	V_{pf} (%)	28-days unit weight (kg/m^3)	f_c (MPa)	f_t (MPa)	f_r (MPa)	Slump flow (mm)
PPFECC1	1	1953	51.3	3.3	3.9	380
PPFECC2	2	1915	44.9	4.3	6.8	340

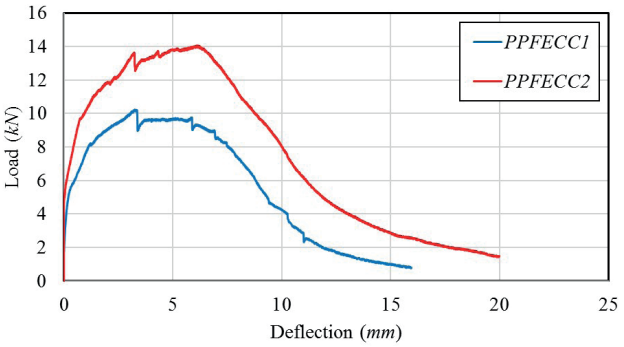

Fig. 8 Load-deflection curves of 300 × 100 × 50 mm beams

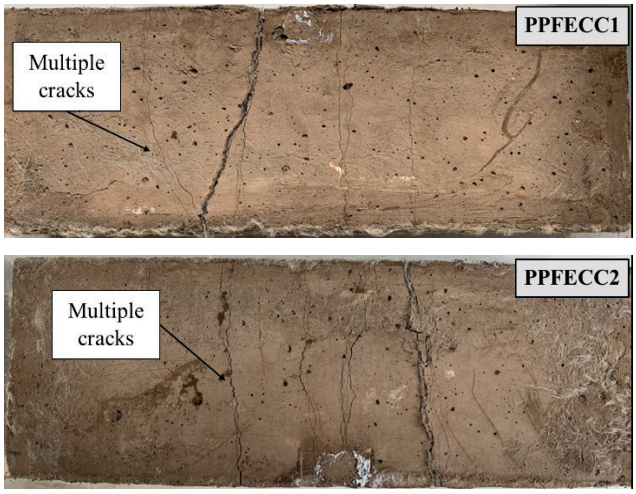

Fig. 9 Multiple micro and macro cracks on the bottom side of PPFECCs

4.2 Analysis of size effect on strength

One of the major influences of size effect parameter is the decrease of strength due to the increase in structure size. Bažant exhibited this parameter by presenting the nominal strength (σ_N) according to the size effect law [19, 21]. The maximum applied loads on both PPFECC mixtures are demonstrated in Table 5. Table 6 shows the results of σ_N derived from Bažant's size effect law for both mixtures.

As shown in Table 6, the σ_N in both PPFECC mixtures decreased when the size of notched beams increased from small (d = 70 mm) to large (d = 280 mm). This decrease in the amount of σ_N due to the increase in beam size indicated the dependence of strength on the size effect parameter. According to Bažant's size effect theory [19, 21], the larger structures release more strain energy to propagate the

Table 5 Maximum applied loads on the PPFECC mixtures

Mixtures	d (mm)	Size	Maximum applied loads (N)		
			Beam 1	Beam 2	Beam 3
PPFECC1	70	Small	2830	2680	3020
	140	Medium	4720	4580	4910
	280	Large	8110	7300	7670
PPFECC2	70	Small	3330	3280	3190
	140	Medium	5110	5620	4840
	280	Large	9310	8770	9240

failure and overcome the fracture process zone compared to the smaller ones; this is the source of size effect on strength. Additionally, it can be seen that the reduction of average value of σ_N due to the increase in the beam size in PPFECC2 with higher tensile ductility was 4% lower than that in PPFECC1. As mentioned earlier, the tensile ductility of PPFECC2 was higher than that of PPFECC1. Therefore, the PPFECC mixture with greater tensile capacity showed a lower size dependency of nominal strength than the one with lower tensile capacity.

4.3 Analysis of size effect on ductility

The size effect on the ductility of structures is another parameter, and Bažant presented this effect through the stress-relative deflection curves for quasi-brittle materials, such as concrete, regarding the energy criterion [19]. Fig. 10 exhibits the load-midspan deflection curves of each geometrically similar notched beam, while Fig. 11 demonstrates stress-relative deflection curves of geometrically similar notched beams for each mixture. Moreover, the crack patterns of these geometrically similar notched beams of PPFECCs are shown in Fig. 12. As shown in Fig. 12, a zone of multiple micro and macro cracks was triggered as the critical crack propagated towards the top of notch, and fine cracks were formed instead of a single crack.

Fig. 10 shows that the resistance and the load-bearing capacity enhanced when the size of notched beams increased from small to large. However, it can be seen in Fig. 11 that each mixture sustained lower stress values and

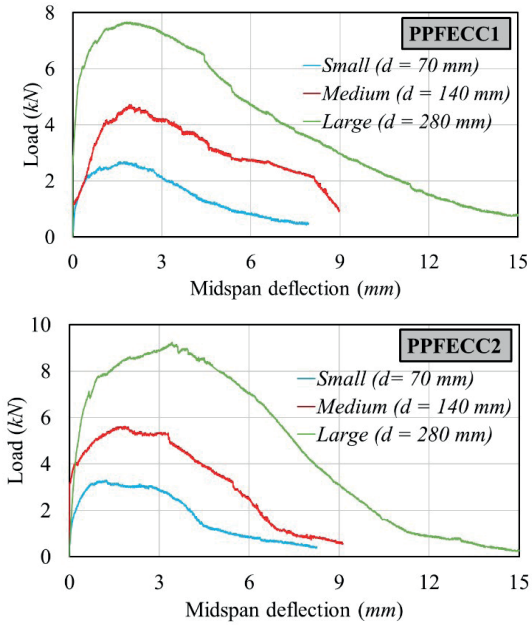

Fig. 10 Load-midspan deflection curves for geometrically similar notched beams

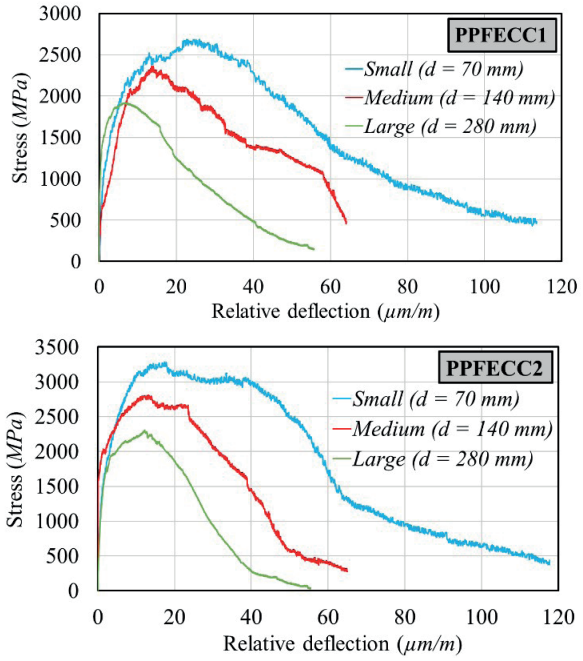

Fig. 11 Stress-relative deflection curves for geometrically similar notched beams

Table 6 Nominal strength (σ_N) in each mixture

Mixtures	f_c (MPa)	f_t (MPa)	Bf_t	Size	d (mm)	d/d_0	σ_{N_1} (MPa)	σ_{N_2} (MPa)	σ_{N_3} (MPa)	$\sigma_{N_{ave}}$ (MPa)	C.V. (%)
PPFECC1	51.3	3.3	0.7	Small	70	0.6	0.58	0.55	0.62	0.58	0.14
				Medium	140	1.1	0.48	0.47	0.51	0.49	0.06
				Large	280	2.3	0.42	0.38	0.4	0.4	0.07
PPFECC2	44.9	4.3	0.8	Small	70	0.4	0.68	0.67	0.65	0.67	0.02
				Medium	140	0.8	0.52	0.58	0.5	0.53	0.22
				Large	280	1.6	0.48	0.45	0.48	0.47	0.04

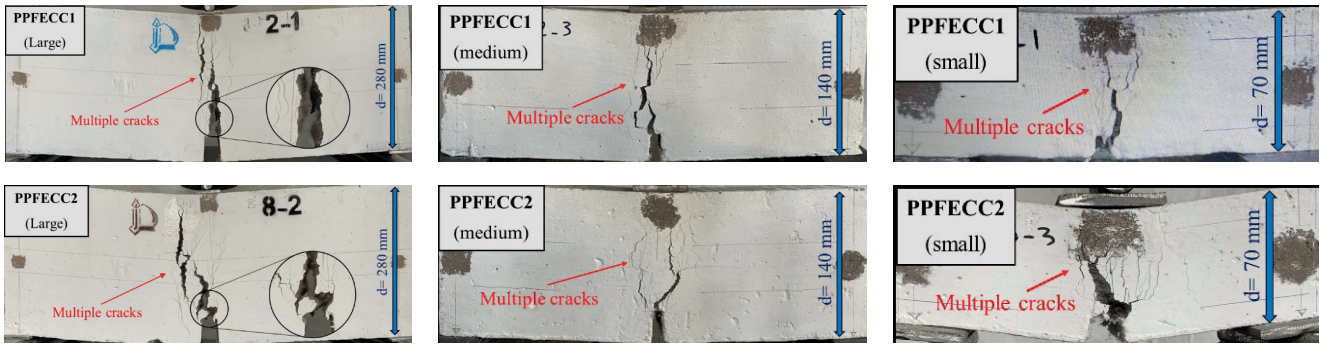

Fig. 12 Crack pattern of geometrically similar notched beams

exhibited less relative deflections as the size of notched beams increased from small to large. This mechanism demonstrates the size effect on the ductility and pre- and post-peak behavior in both PPFECC mixtures. This result is because larger structures release more significant amounts of strain energy to drive the propagation of the failure zone compared to smaller ones [19, 21]. Thus, larger structures exhibited high brittleness and poor ductility compared to small ones in both PPFECC mixtures.

4.4 Analysis of size effect on flexural performance

The equivalent flexural stress versus normalized deflection curves are demonstrated in Fig. 13. The flexural parameters, including equivalent bending strength, deflection, normalized deflection, toughness, and normalized toughness, were averaged from each test result and summarized in Table 7. The toughness and normalized toughness results in Table 7 in each size of notched beams were measured up to the specified deflections for each mixture according to ASTM C1609 [42]. These parameters were measured up to the deflection of $S/50$ for both PPFECC mixtures due to their significant deflections.

The size effect on the equivalent bending strength at LOP and MOR is illustrated in Fig. 14. It can be seen that the f_{LOP} and f_{MOR} decreased in each PPFECC mixture when the size of notched beams increased. This result indicates that the bending strength is sensitive to

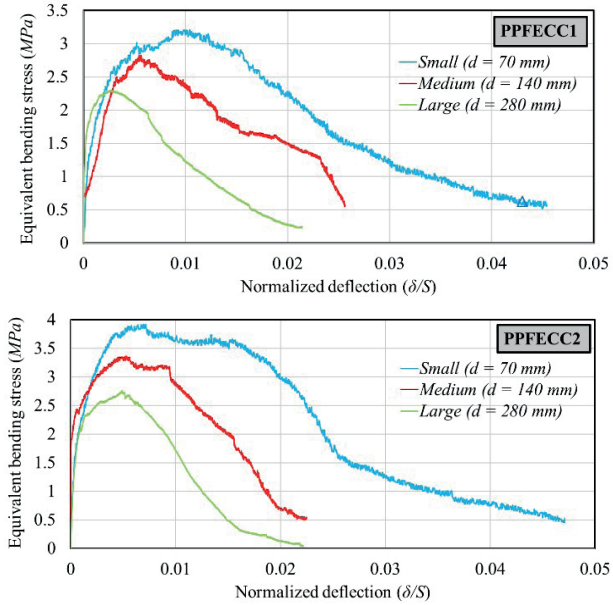

Fig. 13 Average equivalent bending stress (f)-normalized deflection (δ/S) curve

the size of structures and depends on it. The main reason for this mechanism is the amount of released strain energy to propagate failure in structures, which is more significant in large structures compared to small ones [21, 27]. Although both f_{LOP} and f_{MOR} decreased as the size of notched beams increased, this reduction in f_{MOR} was greater than f_{LOP} in both PPFECC mixtures. The same result was reported by Nguyen et al. [27] for ultra-high

Table 7 Average values of flexural parameters and toughness results

Mixtures	f_c (MPa)	f_t (MPa)	Size	d (mm)	δ_{LOP} (mm)	δ_{LOP}/S (%)	f_{LOP} (MPa)	δ_{MOR} (mm)	δ_{MOR}/S (%)	f_{MOR} (MPa)	T (N.m)	T_N(Pa)
PPFECC1	51.3	3.3	Small	70	0.078	0.045	1.7	1.89	1.081	3.4	8.39	57.41
			Medium	140	0.078	0.022	1.39	2.38	0.683	2.83	22.72	38.84
			Large	280	0.076	0.01	1.16	1.98	0.257	2.3	54.43	23.25
PPFECC2	44.9	4.3	Small	70	0.076	0.044	1.74	1.85	0.847	3.85	9.87	67.41
			Medium	140	0.074	0.021	1.66	2.77	0.79	3.1	28.59	48.84
			Large	280	0.079	0.011	1.21	2.81	0.4	2.72	65.13	27.81

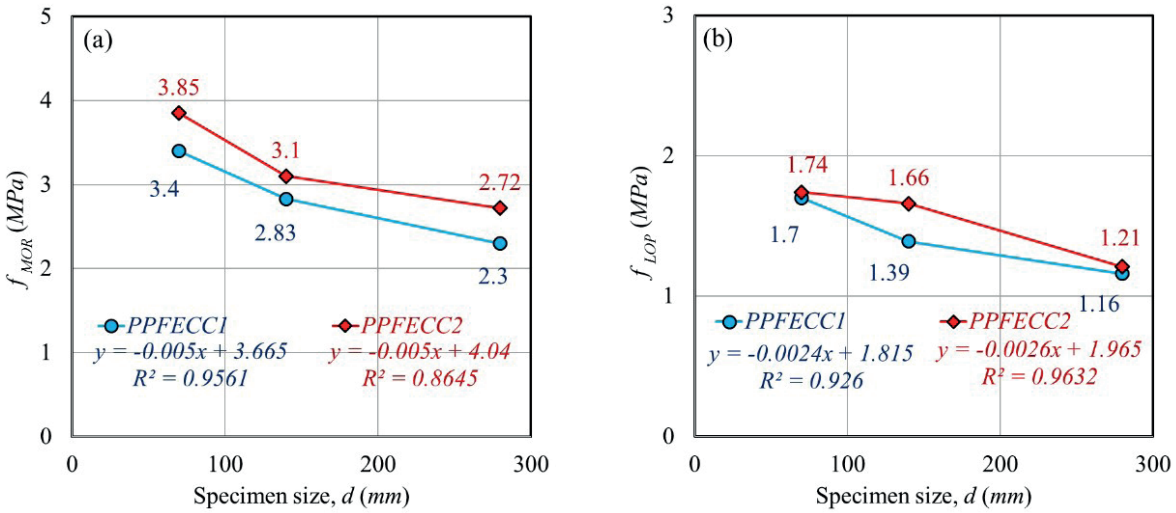

Fig. 14 Size effect on the average equivalent bending stress: (a) at MOR (f_{MOR}) and (b) at LOP (f_{LOP})

performance fiber-reinforced concrete. It can also be seen in Fig. 14 that the reduction of due to the increase in the specimen size from small to large in PPFECC1 was 10.2% higher than that in PPFECC2. It can be concluded that the PPFECC2 with higher tensile ductility showed lower size dependency of bending strength at modulus of rupture compared to PPFECC1 with lower tensile capacity.

The size effect parameter is not only observed for the flexural strength but also for the normalized deflection in Fig. 15. According to Fig. 15, the larger notched beams sustained lower normalized deflections than smaller ones. This is because more strain energy in a larger structure will be released into the crack front than in the smaller one [19]. This strain energy caused the post-peak response to drop steeper and sustain lower amounts of deflection in larger structures than in smaller ones. Moreover,

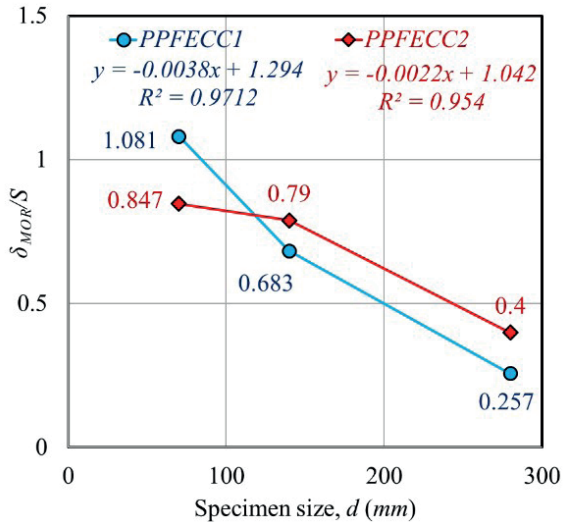

Fig. 15 Size effect on the normalized deflection at MOR (δ_{MOR}/S)

it is observed in Fig. 15 that the reduction of normalized deflection due to the increase in the notched beam size in PPFECC2 with higher tensile ductility was 30.8% lower than that in PPFECC1. Therefore, the significant tensile capacity and development of multiple cracks in PPFECC mixtures showed considerable influence on reducing the severity of size effect on normalized deflection.

According to Table 7, although the toughness (T) increased when the size of notched beams increased to large from small, the normalized toughness (T_N) decreased as the beam size increased from small to large in each mixture. This mechanism in the results of T_N illustrates that the toughness was sensitive to the size of specimens and decreased as the size of specimens increased. The same trend was also reported in the study conducted by Nguyen et al. [27].

4.5 Analysis of size effect on fracture energy

The total fracture energy (G_F) is usually considered a material constant representing the fracture process, including the aggregate interlocking, the bridging mechanism of fibers, and the dissipation mechanism ahead of the notch tip. However, the size effect on G_F has limited it from being considered a material property [32, 47]. In the current study, the determination of size effect on G_F followed RILEM TC-50 FMC [43]. The results of G_F for each mixture are shown in Table 8. According to Table 8, the amounts of G_F in PPFECC1 and PPFECC2 generally increased by 20.6% and 13.8%, respectively, as the size of notched beams increased from small to large. This increase in the amounts of G_F revealed that the fracture energy depended on the size effect parameter. This increase may be attributed to the unwanted absorbed energy out of the

Table 8 Average values of fracture energy in each mixture

Mixtures	f_c (MPa)	f_t (MPa)	f_r (MPa)	Size	d (mm)	w_{t_1} (N.m)	w_{t_2} (N.m)	w_{t_3} (N.m)	$w_{t_{wave}}$ (N.m)	C.V. (%)	G_{F_1} (N/m)	G_{F_2} (N/m)	G_{F_3} (N/m)	$G_{F_{wave}}$ (N/m)
PPFECC1	51.3	3.3	3.9	Small	70	12.39	12.99	14.23	13.2	4.45	3162.1	3313.1	3629.9	3368.5
				Medium	140	29.06	24.68	28.27	27.34	13.3	3706.2	3147.6	3606	3486.6
				Large	280	62.38	59.16	69.47	63.67	29.1	3978.1	3772.8	4430.2	4063.6
PPFECC2	44.9	4.3	6.8	Small	70	17.33	15.68	15.31	16.11	4.79	4420.9	4000	3905.6	4109.3
				Medium	140	33.69	35.28	32.06	33.68	5.13	4297.2	4500	4089.3	4295.7
				Large	280	72.25	71.33	76.43	73.34	6.72	4607.8	4549.1	4874.4	4677.8

fracture process zone and the energy dissipated in the bulk of notched beams, which are much greater in large structures than in small ones [21]. It can also be seen from Table 8 that when the size of specimens enhanced from small to large, the increase in the average value of G_F in PPFECC2 was 33% lower than that in PPFECC1. This result may be due to the higher tensile capacity of PPFECC2 and the development of more multiple cracks in PPFECC2 compared to PPFECC1. Therefore, the tensile ductility and development of multiple cracks effectively decreased the size dependency of fracture energy in PPFECC.

4.6 Size effect parameters of Bažant's size effect theory

Fig. 16 shows Bažant's size effect plot constructed from the experimental data of PPFECC mixtures. Based on Bažant's size effect plot, the behavior of concrete approaches the strength criterion when the ductility of concrete increases and the behavior of concrete approaches the LEFM state when the brittleness of concrete increases [20]. As shown in Fig. 16, the behavior of small size notched beams was closer to the strength criterion, while it approached the LEFM as the size of notched beams increased to large. Thus, the behavior of small size specimens was ductile, and the strength criterion was more appropriate to be utilized for investigating the behavior of small laboratory specimens, while the behavior of large specimens was brittle for each mixture and the LEFM was more rational for designing and analyzing large structures in both PPFECC mixtures.

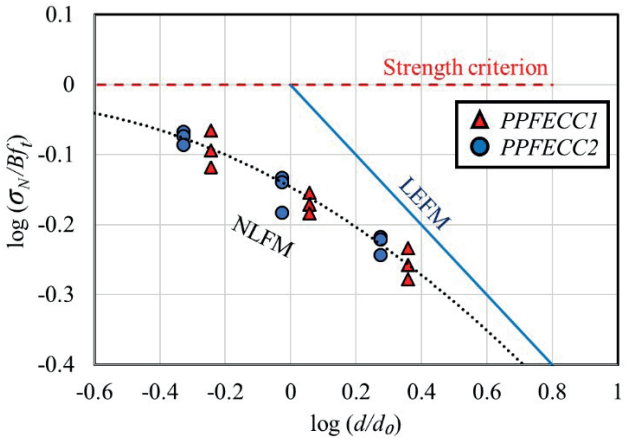

Fig. 16 The size effect plot constructed for PPFECC mixtures

Moreover, as shown in Fig. 16, the results of geometrically similar notched beams in PPFECC2 were located in a more ductile zone than those in PPFECC1. It was apparent that PPFECC2 with higher ductility and tensile strain capacity was closer to the strength criterion and exhibited a lower size effect than PPFECC1 with a lower tensile capacity. Therefore, the tensile ductility in PPFECC suppressed the severity of size effect and shifted the failure mode from brittle fracture to multiple ductile micro and macro cracking.

5 Conclusions

In the current experimental research, the size effect on flexural properties and fracture energy of polypropylene fiber-reinforced engineered cementitious composite (PPFECC) containing local waste materials such as silica fume, electric arc furnace dust, and stone sludge powder was investigated. Two types of PPFECC were prepared: PPFECC1 and PPFECC2, which consist of 1% and 2% dosages of polypropylene fibers, respectively. Both PPFECCs exhibited strain-hardening responses accompanied by multiple micro and macro cracks for geometrically similar notched beams under three-point bending tests. Accordingly, the following conclusions were obtained:

- The nominal strength (σ_N) obtained from Bažant's size effect law for both PPFECC mixtures decreased with the increase in the notched beam size. This decrease in the amount of σ_N indicates the dependence of strength on the size effect parameter in PPFECC. The PPFECC2 with higher tensile ductility produced relatively smaller reductions in σ_N due to the increase in specimen size than PPFECC1.

- According to the stress-relative deflection curves of notched beams, each PPFECC sustained lower stress values and exhibited less relative deflections as the size of notched beams increased. This mechanism shows the severity of size effect on ductility and post-peak softening response in PPFECC.
- Both PPFECC mixtures in flexure exhibited apparent size effect not only on the flexural strength at the limit of proportionality (LOP) and modulus of rupture (MOR) but also on the normalized deflection and the normalized toughness. The higher tensile capacity in PPFECC2 suppressed the severity of size effect on flexural strength more than PPFECC1.
- The fracture energy (G_F) of both PPFECC mixtures was enhanced when the size of notched beams increased. This increase indicates that the values of G_F are size dependent in PPFECCs. On the other hand, the G_F in PPFECC1 with lower tensile capacity showed higher sensitivity to the size effect parameter than PPFECC2.
- According to Bažant's size effect curve, the small size notched beams were close to the strength criterion, while the large ones were close to LEFM in both PPFECCs. However, various sizes of notched beams in PPFECC2 were closer to the strength criterion and were further away from LEFM compared to PPFECC1.

Acknowledgement

The support from Ferdowsi University of Mashhad is gratefully acknowledged.

References

[1] Erdem, T. K. "Specimen size effect on the residual properties of engineered cementitious composites subjected to high temperatures", Cement & Concrete Composites, 45, pp. 1–8, 2014. https://doi.org/10.1016/j.cemconcomp.2013.09.019

[2] Dadmand, B., Pourbaba, M., Riahi, R. "Experimental and Numerical Investigation of Different Types of Jacketing Effect on Retrofitting RC Short Columns Using ECC Concrete", Periodica Polytechnica Civil Engineering, 66(2), pp. 603–613, 2022. https://doi.org/10.3311/PPci.19114

[3] Yu, K., Li, L., Yu, J., Wang, Y., Ye, J., Xu, Q. F. "Direct tensile properties of engineered cementitious composites: A review", Construction and Building Materials, 165, pp. 346–362, 2018. https://doi.org/10.1016/j.conbuildmat.2017.12.124

[4] Dayyani, M., Mortezaei, A., Rouhanimanesh, M. S., Marnani, J. A. "Experimental Study on the Effect of Fibers on Engineered Cementitious Composite Short Square Columns", Periodica Polytechnica Civil Engineering, 66(3), pp. 798–808, 2022. https://doi.org/10.3311/PPci.19612

[5] Krishnaraja, A. R., Kandasamy, S. "Flexural Performance of Hybrid Engineered Cementitious Composite Layered Reinforced Concrete Beams", Periodica Polytechnica Civil Engineering, 62(4), pp. 921–929, 2018. https://doi.org/10.3311/PPci.11748

[6] Turk, K., Demirhan, S. "The mechanical properties of engineered cementitious composites containing limestone powder replaced by microsilica sand", Canadian Journal of Civil Engineering, 40(2), pp. 151–157, 2013. https://doi.org/10.1139/cjce-2012-0281

[7] Li, V. C. "Engineered Cementitious Composites (ECC) Material, structural, and durability performance, concrete construction engineering handbook", In: Nawy, E. G. (ed.) Concrete Construction Engineering Handbook, CRC Press, Chapter 24, 2008. eISBN 9780429127243

[8] da Costa, F. B. P., Righi, D. P., Graeff, A. G., da Silva Filho, L. C. P. "Experimental study of some durability properties of ECC with a more environmentally sustainable rice husk ash and high tenacity polypropylene fibers", Construction and Building Materials, 213, pp. 505–513, 2019. https://doi.org/10.1016/j.conbuildmat.2019.04.092

[9] Zhu, Z., Tan, G., Zhang, W., Wu, C. "Preliminary analysis of the ductility and crack-control ability of engineered cementitious composite with superfine sand and polypropylene fiber (SSPP-ECC)", Materials, 13(11), 2609, 2020. https://doi.org/10.3390/ma13112609

[10] Lan, M., Zhou, J., Xu, M. "Effect of fibre types on the tensile behaviour of engineered cementitious composites", Frontiers in Materials, 8, 775188, 2021. https://doi.org/10.3389/fmats.2021.775188

[11] Jin, H., Li, F., Hu, D. "Research on the flexural performance of reinforced engineered cementitious composite beams", Structural Concrete, 23(4), pp. 2198–2220, 2022. https://doi.org/10.1002/suco.202100012

[12] Fischer, G., Li, V. C. "Effect of matrix ductility on deformation behavior of steel reinforced ECC flexural members under reversed cyclic loading conditions", ACI Structural Journal, 99(6), pp. 781–790, 2002.

[13] Singh, M., Saini, B., Chalak, H. D. "Performance and composition analysis of engineered cementitious composite (ECC) – A review", Journal of Building Engineering, 26, 100851, 2019. https://doi.org/10.1016/j.jobe.2019.100851

[14] Yao, Q., Li, Z., Lu, C., Peng, L., Luo, Y., Teng, X. "Development of engineered cementitious composites using sea sand and metakaolin", Frontiers in Materials, 8, 711872, 2021. https://doi.org/10.3389/fmats.2021.711872

[15] Zhou, J., Qian, S., Beltran, M. G. S., Ye, G., van Breugel, K., Li, V. C. "Development of engineered cementitious composites with limestone powder and blast furnace slag", Materials and Structures, 43, pp. 803–814, 2010. https://doi.org/10.1617/s11527-009-9549-0

[16] Amirfakhrian, S. M. "An experimental investigation on fracture parameters of concrete beams made of engineered cementitious composites (ECC)", Amirkabir Journal of Civil Engineering, 54(8), pp. 1–22, 2022.
https://doi.org/10.22060/CEEJ.2022.19326.7140

[17] Lepech, M., Li, V. C. "Size effect in ECC structural members in flexure", In: Proceedings of 7th International Conference on Fracture Mechanics of Concrete and Concrete Structures (FraMCoS-5), Vail, CO, USA, 2004, pp. 1059–1066. ISBN 0 87031 135 2

[18] Asano, K., Kanakubo, T., Matsushima, T. "Study on size effect in bending behavior of ECC", In: Proceedings of 7th International Conference on Fracture Mechanics of Concrete and Concrete Structures (FraMCoS-7), Jeju, Korea, 2010, pp. 1617–1622. ISBN 978-89-5708-182-2

[19] Bažant, Z. P., Planas, J. "Fracture and size effect in concrete and other quasibrittle materials", Routledge, 1998. 9780203756799
https://doi.org/10.1201/9780203756799

[20] Shah, S. P., Swartz, S. E., Ouyang, C. "Fracture mechanics of concrete: applications of fracture mechanics to concrete, rock, and other quasi-brittle materials", John Wiley and Sons, 1995. ISBN: 978-0-471-30311-4

[21] Bažant, Z. P. "Size effect on structural strength: a review", Archive of Applied Mechanics, 69, pp. 703–725, 1999.
https://doi.org/10.1007/s004190050252

[22] Cifuentes, H., Karihaloo, B. L. "Determination of size-independent specific fracture energy of normal- and high-strength self-compacting concrete from wedge splitting tests", Construction and Building Materials, 48, pp. 548–553, 2013.
https://doi.org/10.1016/j.conbuildmat.2013.07.062

[23] Miarka, P., Pan, L., Bílek, V., Seitl, S., Cifuentés, H. "Influence of the chevron notch type on the values of fracture energy evaluated on alkali-activated concrete", Engineering Fracture Mechanics, 236, 107209, 2020.
https://doi.org/10.1016/j.engfracmech.2020.107209

[24] Karihaloo, B. L., Abdalla, H. M., Imjai, T. "A simple method for determining the true specific fracture energy of concrete", Magazine of Concrete Research, 55(5), pp. 471–481, 2003.
https://doi.org/10.1680/macr.55.5.471.37590

[25] Carpinteri, A., Spagnoli, A. "A fractal analysis of size effect on fatigue crack growth", International Journal of Fatigue, 26, pp. 125–133, 2004.
https://doi.org/10.1016/S0142-1123(03)00142-7

[26] Bažant, Z. P. "Size effect in tensile and compression fracture of concrete structures: computational modeling and design", In: Proceedings of FRAMCOS-3, Gifu, Japan, 1998, pp. 1905–1922.

[27] Nguyen, D. L., Kim, D. J., Ryu, G. S., Koh, K. T. "Size effect on flexural behavior of ultra-high-performance hybrid fiber-reinforced concrete", Composites: Part B, 45, pp. 1104–1116, 2013.
https://doi.org/10.1016/j.compositesb.2012.07.012

[28] Bažant, Z. P. "Size effect", International Journal of Solids and Structures, 37, pp. 69–80, 2000.
https://doi.org/10.1016/S0020-7683(99)00077-3

[29] Pirooznia, A., Moradloo, A. J. "Investigation of size effect and smeared crack models in ordinary and dam concrete fracture tests", Engineering Fracture Mechanics, 226, 106863, 2020.
https://doi.org/10.1016/j.engfracmech.2019.106863

[30] Ghasemi, M., Ghasemi, M. R., Mousavi, S. R. "Studying the fracture parameters and size effect of steel fiber-reinforced self-compacting concrete", Construction and Building Materials, 201, pp. 447–460, 2019.
https://doi.org/10.1016/j.conbuildmat.2018.12.172

[31] Picazo, Á., Alberti, M. G., Gálvez, J. C., Enfedaque, A., Vega, A. C. "The size effect on flexural fracture of polyolefin fibre-reinforced concrete", Applied Sciences, 9(9), 1762, 2019.
https://doi.org/10.3390/app9091762

[32] Sim, J.-I., Yang, K.-H., Lee, E.-T., Yi, S.-T. "Effects of aggregate and specimen sizes on lightweight concrete fracture energy", Journal of Materials in Civil Engineering, 26(5), pp. 845–854, 2014.
https://doi.org/10.1061/(ASCE)MT.1943-5533.0000884

[33] Zhang, D., Wu, K. "Fracture process zone of notched three point-bending concrete beams", Cement and Concrete Research, 29(12), pp. 1887–1892, 1999.
https://doi.org/10.1016/S0008-8846(99)00186-6

[34] Carpinteri, A., Chiaia, B. "Multifractal nature of concrete fracture surfaces and size effects on nominal fracture energy", Materials and Structures, 28, pp. 435–443, 1995.
https://doi.org/10.1007/BF02473162

[35] Carpinteri, A., Chiaia, B. "Size effects on concrete fracture energy: dimensional transition from order to disorder", Materials and Structures, 29, pp. 259–266, 1996.
https://doi.org/10.1007/BF02486360

[36] Guinea, G. V., Planas, J., Elices, M. "Measurement of the fracture energy using three-point bend tests: part 1- influence of experimental procedures", Materials and Structures, 25, pp. 212–218, 1992.
https://doi.org/10.1007/BF02473065

[37] Planas, J., Elices, M., Guinea, G. V. "Measurement of the fracture energy using three-point bend tests: part 2- influence of bulk energy dissipation", Materials and Structures, 25, pp. 305–312, 1992.
https://doi.org/10.1007/BF02472671

[38] Elices, M., Guinea, G. V., Planas, J. "Measurement of the fracture energy using three-point bend tests: part 3- influence of cutting the P-δ tail", Materials and Structures, 25, pp. 327–334, 1992.
https://doi.org/10.1007/BF02472591

[39] Sabzi, J., Shamsabadi, E. A., Ghalehnovi, M., Hadigheh, S. A., Khodabakhshian, A., de Brito, J. "Mechanical and durability properties of mortars incorporating red mud, ground granulated blast furnace slag, and electric arc furnace dust", Applied Sciences, 11(9), 4110, 2021.
https://doi.org/10.3390/app11094110

[40] Shah, S. P. "Size-effect method for determining fracture energy and process zone size of concrete", Materials and Structures, 23(6), pp. 461–465, 1990,
https://doi.org/10.1007/BF02472030

[41] BS EN14651 "Test method for metallic fibre concrete-measuring the flexural tensile strength (Limit of Proportionality (LOP), Residual)", The British Standards Institution, London, UK, 2007.
https://doi.org/10.3403/30092475U

[42] ASTM C1609/C1609M-12 "Standard test method for flexural performance of fiber-reinforced concrete (using beam with third-point loading)", American Society of Testing and Materials, West Conshohocken, PA, USA, 2012.
https://doi.org/10.1520/C1609_C1609M-12

[43] RILEM TC-50 FMC "Determination of the fracture energy of mortar and concrete by means of three-point bend tests on notched beams", Materials and Structures, 18(4), pp. 287–290, 1985. https://doi.org/10.1007/BF02472918

[44] BS EN 12390 "Testing hardened concrete. method of determination of compressive strength of concrete cubes, (BS, Part 3)", British Standards Institution, London, UK, 2009. https://doi.org/10.3403/30164906

[45] ASTM "ASTM C78/C78M-10 Standard test method for flexural strength of concrete (using simple beam with third-point loading)", American Society of Testing and Materials, West Conshohocken, PA, USA, 2010. https://doi.org/10.1520/C0078_C0078M-10

[46] ASTM C496/C496M-04e1 "Standard test method for splitting tensile strength of cylindrical concrete specimens", American Society of Testing and Materials, West Conshohocken, PA, USA, 2011. https://doi.org/10.1520/C0496_C0496M-04E01

[47] Hillerborg, A., Modéer, M., Petersson, P.-E. "Analysis of crack formation and crack growth in concrete by means of fracture mechanics and finite element", Cement and Concrete Research, 6(6), pp. 773–781, 1976. https://doi.org/10.1016/0008-8846(76)90007-7